

Bandwidth enhancement of MIR emission in $\text{Yb}^{3+}/\text{Er}^{3+}/\text{Dy}^{3+}$ triply doped fluoro-tellurite glass

This content has been downloaded from IOPscience. Please scroll down to see the full text.

2017 Laser Phys. Lett. 14 035804

(<http://iopscience.iop.org/1612-202X/14/3/035804>)

View [the table of contents for this issue](#), or go to the [journal homepage](#) for more

Download details:

IP Address: 134.148.10.13

This content was downloaded on 09/02/2017 at 06:35

Please note that [terms and conditions apply](#).

You may also be interested in:

[The effects of \$\text{Ho}^{3+}\$ and \$\text{Pr}^{3+}\$ ions on the spectroscopic properties of \$\text{Er}^{3+}\$ doped \$\text{SrGdGa}_3\text{O}_7\$ crystals used in mid-infrared lasers](#)

Houping Xia, Jianghe Feng, Yan Wang et al.

[Multi-modal luminescence properties of \$\text{RE}^{3+}\$ \(\$\text{Tm}^{3+}\$, \$\text{Yb}^{3+}\$ \) and \$\text{Bi}^{3+}\$ activated \$\text{GdNbO}_4\$ phosphors—upconversion, downshifting and quantum cutting for spectral conversion](#)

A Dwivedi, Kavita Mishra and S B Rai

[Spectroscopic properties of \$\text{Er}^{3+}\$ and \$\text{Yb}^{3+}\$ co-doped glass ceramics containing \$\text{SrF}_2\$ nanocrystals](#)

Xvsheng Qiao, Xianping Fan, Minquan Wang et al.

[Intense white light emission in \$\text{Tm}^{3+}/\text{Er}^{3+}/\text{Yb}^{3+}\$ co-doped \$\text{Y}_2\text{O}_3\text{-ZnO}\$ nano-composite](#)

R S Yadav, R K Verma and S B Rai

[\$\text{Er}^{3+}\$ and \$\text{Yb}^{3+}\$ concentration effect in \$\text{Yb}^{3+}/\text{Er}^{3+}\$ codoped tellurite glasses](#)

H Desirena, E De la Rosa, A Shulzgen et al.

[Spectral analysis of \$\text{Er}^{3+}\$ -, \$\text{Er}^{3+}/\text{Yb}^{3+}\$ - and \$\text{Er}^{3+}/\text{Tm}^{3+}/\text{Yb}^{3+}\$ -doped \$\text{TeO}_2\text{-ZnO-WO}_3\text{-TiO}_2\text{-Na}_2\text{O}\$ glasses](#)

G Lakshminarayana, Jianrong Qiu, M G Brik et al.

[Infrared to visible up-conversion study](#)

N Jaba, A Kanoun, H Mejri et al.

[A fruitful demonstration in sensors based on upconversion luminescence of \$\text{Yb}^{3+}/\text{Er}^{3+}\$ codoped \$\text{Sb}_2\text{O}_3\text{-WO}_3\text{-Li}_2\text{O}\$ \(SWL\) glass-ceramic](#)

Prasenjit Prasad Sukul and Kaushal Kumar

Letter

Bandwidth enhancement of MIR emission in $\text{Yb}^{3+}/\text{Er}^{3+}/\text{Dy}^{3+}$ triply doped fluoro-tellurite glass

Sathravada Balaji, Amarnath R Allu, Kaushik Biswas, Gaurav Gupta, Debarati Ghosh and Kalyandurg Annapurna

GSTS, CSIR-Central Glass and Ceramic Research Institute, Kolkata—700 032, India

E-mail: sbalaji@cgcri.res.in and annapurnak@cgcri.res.in

Received 2 December 2016, revised 22 January 2017

Accepted for publication 23 January 2017

Published 8 February 2017



CrossMark

Abstract

Enhanced bandwidth of MIR emission from $\text{Yb}^{3+}/\text{Er}^{3+}/\text{Dy}^{3+}$ triply doped low phonon oxide glass system has been reported in this work. With considerable gain cross-section, the MIR emission bandwidth can be stretched from ~ 2600 to 3100 nm (~ 500 nm) which is practically not possible to obtain from Er^{3+} or Dy^{3+} ions singly doped systems. Co-doping of Dy^{3+} ions not only quenches the unfavourable visible up-converted emissions from Er^{3+} ions but also mitigates the prominent ~ 1.5 μm emission. A broad MIR emission on superimposition of Er^{3+} ~ 2.76 μm and Dy^{3+} ~ 2.95 μm emissions was obtained owing to the efficient energy transfer (ET) $\text{Yb}^{3+} \rightarrow \text{Er}^{3+} \rightarrow \text{Dy}^{3+}$ upon ~ 980 nm excitation. The present glasses can be fiberized to develop compact and tunable MIR solid state fiber laser sources.

Keywords: broadband, Yb^{3+} , tellurite glass, MIR emission, Er^{3+} , Dy^{3+}

(Some figures may appear in colour only in the online journal)

1. Introduction

Efficient, compact and broad band solid state laser sources in the mid-infrared (MIR) region of wavelengths between ~ 2 – 5 μm are highly essential to trace low level air pollutants/green-house gases or even the human breath for the purpose of medical diagnostics. MIR lasers (~ 2.5 – 3 μm) also show enormous applications in tissue engineering/surgery [1]. Currently available MIR laser sources based on optical non-linear conversion techniques such as OPOs (optical parametric oscillator) and DFGs (difference frequency generation) are very complex, expensive and also not compact [2]. Expensive semiconductor based quantum cascade lasers (QCL) provide a narrow tuning range (~ 140 cm^{-1}) with low wall plug efficiencies and adjacent cryo-cooling setup [1, 3] is again a cost additive process. Although, transition metal ion-doped chalcogenide-based crystals lasing in the broad ~ 2 – 3 μm region are available [1, 4, 5], thermal lensing is the main concern

which limits high peak powers [6]. As such crystals have some unavoidable limitations compared to glasses such as the costly preparation techniques, non required size and shape etc. In this scenario, trivalent lanthanides (Ln^{3+}) doped oxide glasses lasing in the MIR region have distinct advantages including their cost-effective preparation and no constraints on size and shape compared to the above mentioned sources.

Ln^{3+} ions are familiar for their emission characteristics starting from UV to MIR region are highly host material phonon energy dependent. However, Ln^{3+} ions are known for their narrow emission band widths of typically 100 – 150 cm^{-1} but possess very high average peak powers. Ln^{3+} doped MIR transparent fluoride [1, 7–12] and chalcogenide [1, 2, 13, 14] based glasses are widely explored for their MIR emission properties, nevertheless, these glasses are known for their poor chemical, thermal and mechanical stability than oxide glasses. In the current decade, much progress evolved on the low phonon (~ 750 cm^{-1}) tellurium oxide based glasses and

even fibers are commercially available which are transparent up to $\sim 5 \mu\text{m}$ [15]. Ln^{3+} ions such as Er^{3+} [14, 16–20], Ho^{3+} [21–23], Dy^{3+} [24–26] doped tellurite glasses are rigorously explored for the development of efficient MIR solid state laser sources. To enhance the absorption pump power at the excitation wavelength so as to increase the efficiency of MIR emissions, co-doping of Ln^{3+} ions have been reported [10, 19, 20, 23, 27–31] in a variety of host materials and in fact it showed better results compared to Ln^{3+} ions' singly doped systems. However, to the best of our knowledge, there are no studies/reports on the bandwidth enhancement of MIR emission in combination of Ln^{3+} ions.

Herein, we explored the combination of rare earths such as Er^{3+} ions (MIR emission maxima at $\sim 2.76 \mu\text{m}$) and Dy^{3+} ions (MIR emission maxima at $\sim 2.95 \mu\text{m}$) in a low phonon ($\sim 650 \text{cm}^{-1}$) fluoro-tellurite glass system to see the viability on the bandwidth enhancement with considerable gain cross-section. To enhance the absorption cross-section at the excitation wavelength, $\sim 980 \text{nm}$, Yb^{3+} ions were doped with $\text{Er}^{3+}/\text{Dy}^{3+}$ co-doped glass system. To understand the energy transfer (ET) dynamics on the enhancement of emission intensity/bandwidth; Er^{3+} , Dy^{3+} singly doped, $\text{Er}^{3+}/\text{Yb}^{3+}$, $\text{Dy}^{3+}/\text{Yb}^{3+}$ co-doped fluoro-tellurite glass systems were also prepared and studied in detail upon 976nm laser diode excitation. A broad $\sim 279 \text{nm}$ MIR emission with considerable gain cross-section has been recorded for the first time in an $\text{Yb}^{3+}/\text{Er}^{3+}/\text{Dy}^{3+}$ triply doped tellurite glass system to the best of our knowledge.

2. Material and methods

Fluoro-Tellurite glass with the chemical composition (mol%) $75\text{TeO}_2-15\text{BaF}_2-5\text{AlF}_3-5\text{LaF}_3$ has been considered for the active rare earth ion doping in view of its good glass forming ability, better thermal, chemical and mechanical properties (not part of the present study). The active ions such as Er^{3+} , Yb^{3+} and Dy^{3+} were substituted partially for La^{3+} . The as-designed new glasses were prepared using the melt quenching technique as described elsewhere [32]. The glass samples have been labelled in accordance with the active ion present in the chemical composition of glass as given below:

Er: 75% $\text{TeO}_2-15\%$ $\text{BaF}_2-5\%$ $\text{AlF}_3-4\%$ $\text{LaF}_3-1\%$ ErF_3

ErYb: 75% $\text{TeO}_2-15\%$ $\text{BaF}_2-5\%$ $\text{AlF}_3-3\%$ $\text{LaF}_3-1\%$ $\text{ErF}_3-1\%$ YbF_3

ErDyYb: 75% $\text{TeO}_2-15\%$ $\text{BaF}_2-5\%$ $\text{AlF}_3-2.5\%$ $\text{LaF}_3-1\%$ $\text{ErF}_3-1\%$ $\text{YbF}_3-0.5\%$ DyF_3

Dy: 75% $\text{TeO}_2-15\%$ $\text{BaF}_2-5\%$ $\text{AlF}_3-4.5\%$ $\text{LaF}_3-0.5\%$ DyF_3

DyYb: 75% $\text{TeO}_2-15\%$ $\text{BaF}_2-5\%$ $\text{AlF}_3-3.5\%$ $\text{LaF}_3-0.5\%$ $\text{DyF}_3-1\%$ YbF_3 .

The concentration of individual dopant active ions (Er^{3+} , Yb^{3+} , Dy^{3+}) was fixed after careful analysis of luminescence quenching properties when each single ion was doped with increasing concentration (not shown in the present work). Spectral measurements were performed on optically polished $\sim 2 \text{mm}$ thick glass samples at room temperature (RT). The experimental techniques to record the absorption, emission,

excitation spectra and fluorescence decay kinetics of the samples using appropriate filters both at excitation and emission channels were described elaborately elsewhere [23]. The visible upconversion (Vis-UC) emission spectra of all the samples were recorded in a similar condition using 976nm fiber pigtailed laser diode (Model: BL-976 PAG900) supplied by Thorlabs, USA.

3. Results and discussion

3.1. Absorption spectral analysis

The absorption spectra presented in figure 1, depicts distinct absorption transitions [33] of Er^{3+} , Dy^{3+} and Yb^{3+} ions in singly doped, co-doped and triply doped glass samples. Insets (a) and (b) of figure 1 present the spectral overlap of absorption bands corresponding to Yb^{3+} , Er^{3+} , Dy^{3+} ions in the excitation wavelength region $\sim 980 \text{nm}$ and spectral overlap nature of Er^{3+} and Dy^{3+} ions in region of $1400-1900 \text{nm}$ respectively. Yb^{3+} ions with high absorption cross-section at the excitation wavelength ($\sim 980 \text{nm}$) as well as excellent spectral overlap with activators Er^{3+} , Dy^{3+} ions have distinct advantages in obtaining enhanced NIR (near infrared)/MIR emission properties. In the present glass with phonon energy $\sim 650 \text{cm}^{-1}$, ET from $\text{Yb}^{3+} \rightarrow \text{Dy}^{3+}$ or $\text{Er}^{3+} \rightarrow \text{Dy}^{3+}$ may hardly require less than a phonon energy, which ensures an efficient ET from Yb^{3+} donor to Er^{3+} and Dy^{3+} acceptor ions which has been discussed in the following sections.

3.2. MIR luminescence and ET dynamics

MIR luminescent measurements are very critical since the higher order harmonics of the excitation wavelength falls exactly at the MIR luminescence region of active ions. For example, if the excitation is at 800nm then a fourth order harmonic peak appears at $\sim 3200 \text{nm}$ and if $\sim 980 \text{nm}$ is the excitation wavelength then a third order harmonic peak appears at $\sim 2940 \text{nm}$ which are very close to the MIR emission transitions of Ho^{3+} ($\sim 2.85 \mu\text{m}$), Er^{3+} ($\sim 2.76 \mu\text{m}$), Dy^{3+} ($\sim 2.95 \mu\text{m}$) ions. There are such erroneous reports in low phonon oxide based glasses with considerable OH^- content in the glass [26, 34, 35]. In this study, the MIR emission spectrum was recorded at RT with utmost care using proper low and high pass filters at the excitation and emission channels respectively as described elsewhere [23]. Figure 2(a) presents the MIR emission spectrum corresponding to the $\text{Er}^{3+}:^4\text{I}_{11/2} \rightarrow ^4\text{I}_{13/2}$ transition in Er^{3+} singly doped (Er) and $\text{Er}^{3+}/\text{Yb}^{3+}$ co-doped (ErYb) samples. Figure 2(b) presents the MIR emission spectrum of $\text{Er}^{3+}/\text{Dy}^{3+}/\text{Yb}^{3+}$ (ErDyYb) triply doped glass along with Dy^{3+} ions singly doped (Dy) and $\text{Dy}^{3+}/\text{Yb}^{3+}$ co-doped (DyYb) samples for comparison of the relative emission intensities. The MIR emission transition in the ErDyYb sample corresponds to both Er^{3+} ($^4\text{I}_{11/2} \rightarrow ^4\text{I}_{13/2}$) and Dy^{3+} ($^6\text{H}_{13/2} \rightarrow ^6\text{H}_{15/2}$) emission transitions. The MIR emission spectrum was authenticated by the excitation spectrum which was recorded by monitoring the respective MIR emission transition corresponding to the rare earth ions (Er^{3+} , Dy^{3+}) and has been presented in figures 2(a)

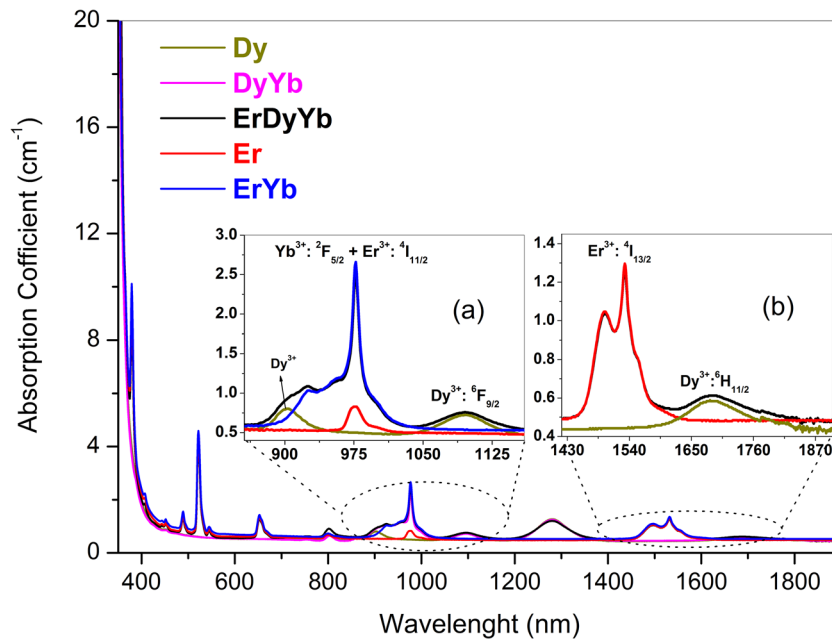


Figure 1. Absorption spectra of Er^{3+} , Dy^{3+} and Yb^{3+} ions in doped/co-doped glass systems. Inset (a): spectral overlap nature in the excitation wavelength region ($\sim 980\text{nm}$); inset (b): spectral overlap of Er^{3+} and Dy^{3+} ions around $\sim 1550\text{nm}$.

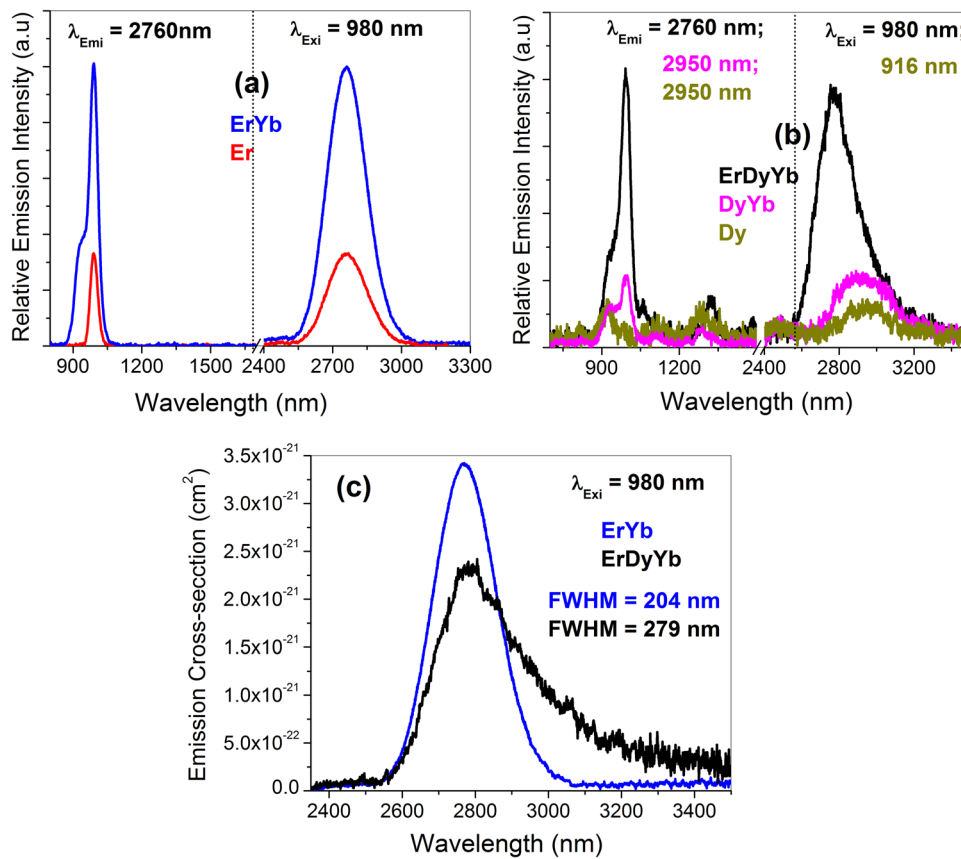


Figure 2. (a) and (b) MIR emission and excitation spectra (c) emission cross-section spectra derived using the FL method.

and (b) itself. The emission cross-section spectra calculated using the Fuchtbauer and Ladenburg (FL) method and the corresponding full width at half maximum (FWHM) values for ErYb and ErDyYb samples are presented in figure 2(c).

$\text{Er}^{3+}/\text{Yb}^{3+}$ ions co-doped systems are familiar for their efficient NIR $\sim 1.5\ \mu\text{m}$ emission as well as Vis-UC emission

properties [36–38]. These emission properties are highly dependent on the Er^{3+} ion concentration as well as on the excitation (980nm) laser intensity. A detailed study on the influence of Er^{3+} ion concentration ($0.5\text{--}3\ \text{mol}\%$ with fixed $1\ \text{mol}\%$ of Yb^{3+} ions) and $980\ \text{nm}$ laser excitation pump power on the Vis-UC emission properties in the present studied glass

host indicates the upconversion favourable energy transfer upconversion (ETU) process from ${}^4I_{11/2}$ as well as ${}^4I_{13/2}$ levels enhanced to a great extent at higher concentrations and even at low concentrations provided at higher pump powers. Quenching of MIR emission intensity for Er^{3+} ion concentration >1 mol% has been observed in the present host glass. Hence the ErYb sample co-doped with 1 mol% of Er^{3+} and Yb^{3+} ions has been considered for MIR emission spectral analysis. In the case of Er^{3+}/Yb^{3+} co-doped systems, the energy transfer (ET) and back transfer (EBT) among resonant $Yb^{3+}:{}^2F_{5/2} \leftrightarrow Er^{3+}:{}^4I_{11/2}$ excited states are vital, as already said ErYb (1 mol %) is the optimised sample for efficient $\sim 2.7 \mu m$ emission; but, this concentration also shows enhanced Vis-UC emissions and prominent $\sim 1.5 \mu m$ emission compared to the Er sample. To mitigate the Vis-UC as well as prominent $\sim 1.5 \mu m$ emission from Er^{3+} ions, attempts were made by co-doping with Pr^{3+} , Nd^{3+} , Ho^{3+} and Tm^{3+} ions in the number of glasses/crystals (having low phonon energy) to enhance the $\sim 2.7 \mu m$ emission from ${}^4I_{11/2}$ state [19, 20, 27, 31, 39]. Since, the lifetime of $Er^{3+}:{}^4I_{13/2}$ level ($\sim 1.5 \mu m$) is in the order of few 'ms', fast depopulation of this level is highly essential to enhance the population density and rate at ${}^4I_{11/2}$ state so as to increase the efficiency of Er^{3+} $\sim 2.7 \mu m$ emission. Co-doping with Ho^{3+} [31], Tm^{3+} [27] ions may restrict the Er^{3+} : $\sim 1.5 \mu m$ emission to some extent. However, the energy level structure of Ho^{3+} and Tm^{3+} ions would promote the Vis-UC emission properties not only from Er^{3+} ions but also from Ho^{3+} and Tm^{3+} ions alongside the enhancement of NIR emissions from Ho^{3+} ($\sim 2 \mu m$) and Tm^{3+} ($\sim 1.8 \mu m$) ions. Again in the presence of Yb^{3+} ions these effects would be at higher side as $Yb^{3+} \rightarrow Ho^{3+}$ and $Yb^{3+} \rightarrow Tm^{3+}$ ET shows enhanced Vis-UC/NIR emission properties in the number of tellurite glass systems. On the other hand, Pr^{3+} ions co-doped [20, 39] systems have been reported with reduced Vis-UC as well as $\sim 1.5 \mu m$ emission characteristics from Er^{3+} ions. But, there are no reports on Dy^{3+} ions co-doping effects on MIR emission properties other than enhancement of green UC emission upon 800 nm excitation [40] in Er^{3+}/Dy^{3+} co-doped $LiNbO_3$ crystal. Dy^{3+} ions possess a broad MIR emission [7], nevertheless, the predominant multi phonon non-radiative relaxations (MPR) from closely packed (which are separated apart few 100 cm^{-1}) multiple excited states greatly quenches the MIR emission from Dy^{3+} ions in low phonon oxide based glass systems. Taking advantage of the broadness from Dy^{3+} ions and peak intensity from Er^{3+} ions, we attempted to study the MIR emission properties assuming a broad and intense MIR emission from Er^{3+}/Dy^{3+} ions upon 980 nm excitation of Yb^{3+} ions (advantage of Yb^{3+} ions co-doping were discussed elsewhere [23]). Moreover, there are no reports on the bandwidth enhancement of MIR emission neither from Pr^{3+} nor from Ho^{3+} , Tm^{3+} co-doped systems.

As shown in figure 2(b), a less intense MIR emission band from Dy^{3+} ions singly doped glass upon 916 nm excitation having FWHM of $\sim 320 \text{ nm}$ has been recorded which is broader than TZN ($\text{TeO}_2\text{-ZnO-Na}_2\text{O}$)/TZNF ($\text{TeO}_2\text{-ZnO-Na}_2\text{O-ZnF}_2$) ($\sim 290 \text{ nm}$) tellurium oxide based glasses [25] and probably the highest value reported so far if not compared/considered with a super broad ($\sim 650 \text{ nm}$) MIR emission

from Dy^{3+} ions [26] from TZN (tellurite) and GPNG ($\text{GeO}_2\text{-PbO-Na}_2\text{O-Ga}_2\text{O}_3$) (germanate) oxide based glasses as the results are seems to be speculative. In the presence of Yb^{3+} ions, a considerable effect on the enhancement of MIR emission intensity from ErYb and DyYb samples compared to Er^{3+} and Dy^{3+} singly doped glasses have been observed (figures 2(a) and (b)). Nevertheless $Er^{3+}/Dy^{3+}/Yb^{3+}$ triply doped glass (ErDyYb) shows decreased emission intensity compared to the ErYb sample; the broadness (FWHM) of the band has been increased from 204 to 279 nm. Also, compared to Dy and DyYb samples, a ~ 4 fold enhancement in the MIR emission intensity has been noticed in the ErDyYb sample. The emission cross-section values in the order of 10^{-21} cm^2 are comparable to other reported host materials [9, 16, 18, 19, 29, 41] but, the FWHM values are better than any other host material. The observed broadness can be attributed to two reasons: first, the presence of different structural units in the tellurite glass will lead to inhomogeneous broadening of the emission band is well known and articulated in the literature [42–44] and the second reason is due to the excellent MIR emission spectral overlap (inset (b) of figure 1) of Er^{3+} and Dy^{3+} ions with efficient $Er^{3+} \rightarrow Dy^{3+}$ ET process in the present glass as depicted through an energy level diagram in figure 3.

The excellent spectral overlap nature of Yb^{3+} with Er^{3+} and Dy^{3+} ions in the present case as shown in figure 1, may hardly require less than a phonon energy of the host material in the case of $Yb^{3+}:{}^2F_{5/2} \rightarrow Dy^{3+}:{}^6F_{9/2}$ and $Yb^{3+}:{}^2F_{5/2} \leftrightarrow Er^{3+}:{}^4I_{11/2}$ is in good resonance to ensure an efficient ET from Yb^{3+} ions upon 980 nm excitation as described below.

ErYb: $Yb^{3+} ({}^2F_{5/2}) \rightarrow Er^{3+} ({}^4I_{11/2}) \Rightarrow Er^{3+}:{}^4I_{11/2} \rightarrow {}^4I_{13/2}$
(2.76 μm)

DyYb: $Yb^{3+} ({}^2F_{5/2}) \rightarrow Dy^{3+} ({}^6H_{7/2}) + \text{MPR} ({}^6F_{9/2} + {}^6F_{11/2} + {}^6H_{11/2} + {}^6H_{13/2}) \Rightarrow Dy^{3+}:{}^6H_{13/2} \rightarrow {}^6H_{15/2}$ (2.95 μm)

ErDyYb:

(1) ErYb (2.76 μm) + $Er^{3+} ({}^4I_{11/2}) \rightarrow Dy^{3+} ({}^6H_{7/2}) + \text{MPR} \Rightarrow Dy^{3+}:{}^6H_{13/2} \rightarrow {}^6H_{15/2}$ (2.95 μm)

(2) ErYb (2.76 μm) + $Er^{3+} ({}^4I_{13/2}) \rightarrow Dy^{3+} ({}^6H_{11/2}) + \text{MPR} \Rightarrow Dy^{3+}:{}^6H_{13/2} \rightarrow {}^6H_{15/2}$ (2.95 μm).

To understand the above interpreted ET paths and its efficiency, NIR emission properties of Er^{3+} ions were investigated in the presence of Yb^{3+} and Dy^{3+} ions. Figure 4 presents the NIR emission spectra of Er^{3+} ions and its influence in the presence of Yb^{3+} and Dy^{3+} ions at RT. We have not observed any Dy^{3+} related NIR emission bands at $\sim 1.15 \mu m$, $\sim 1.3 \mu m$ and $\sim 1.7 \mu m$ [13] due to the dominance of MPR rate which is totally related to the maximum phonon energy of the host material. Insets (a) and (b) of figure 4 represent the decay profiles of 1006 nm corresponding to both $Yb^{3+}:{}^2F_{5/2} \rightarrow {}^2F_{7/2}$ as well as $Er^{3+}:{}^4I_{11/2} \rightarrow {}^4I_{15/2}$ transition and 1570 nm corresponding to $Er^{3+}:{}^4I_{13/2} \rightarrow {}^4I_{15/2}$ emission transition respectively for the samples.

The advantage of Yb^{3+} ions is clearly witnessed with the enhanced NIR emission and decay times of $Er^{3+}:{}^4I_{11/2}$ as well as ${}^4I_{13/2}$ states over Er^{3+} ions singly doped glass. In the ErDyYb sample, as evidenced from figure 4, the emission intensity of Yb^{3+} ions (1006 nm: ~ 10 folds) as well as Er^{3+} ions (1570 nm: ~ 60 folds) drastically quenched compared to

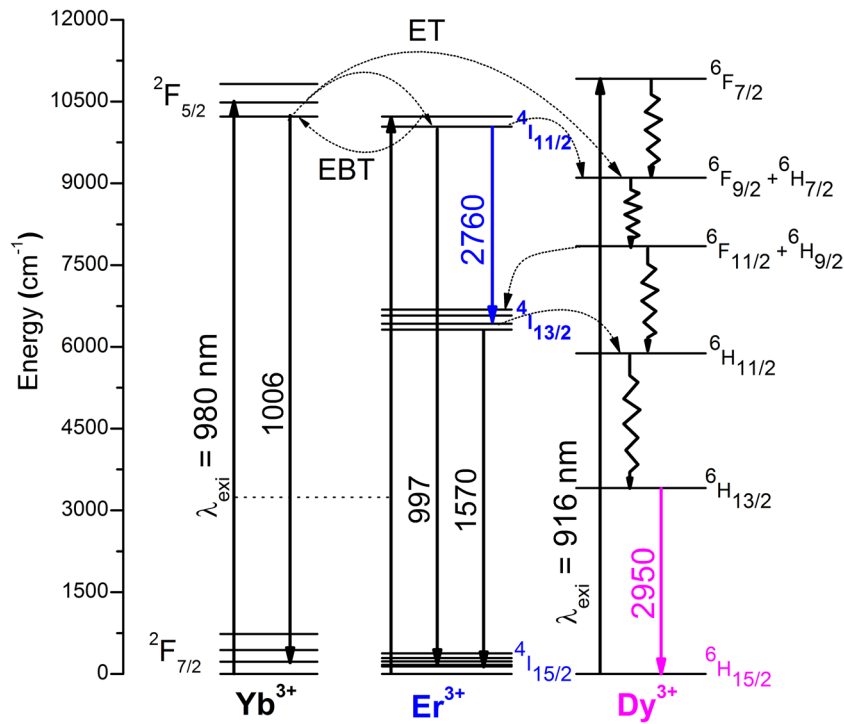


Figure 3. Energy level diagram depicting the MIR emission transition from Er³⁺ and Dy³⁺ ions upon Yb³⁺ ion excitation.

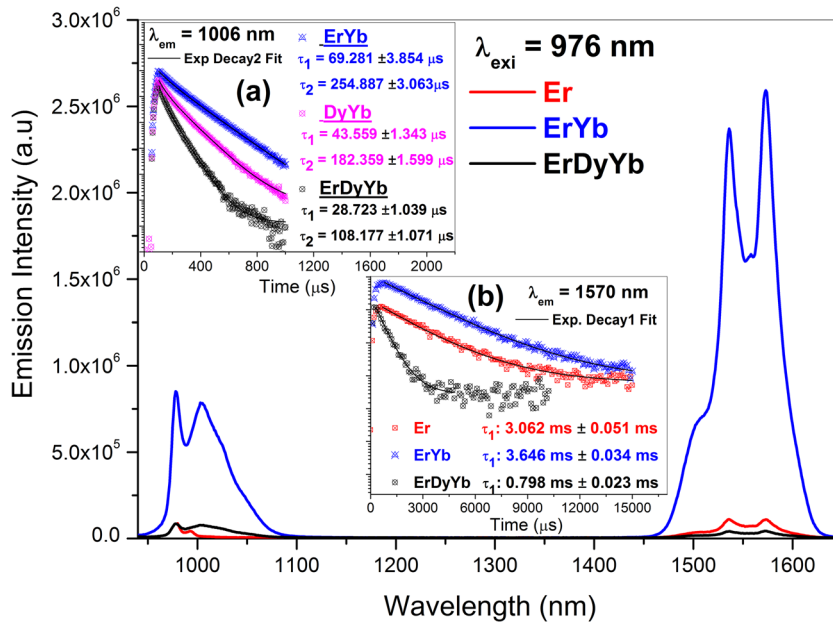


Figure 4. NIR emission of Er³⁺ ions in presence of Yb³⁺ and Dy³⁺ ions. Inset (a): decay profiles of 1006 nm emission fitted to double exponential function; inset (b): decay profiles of 1570 nm emission fitted to single exponential function.

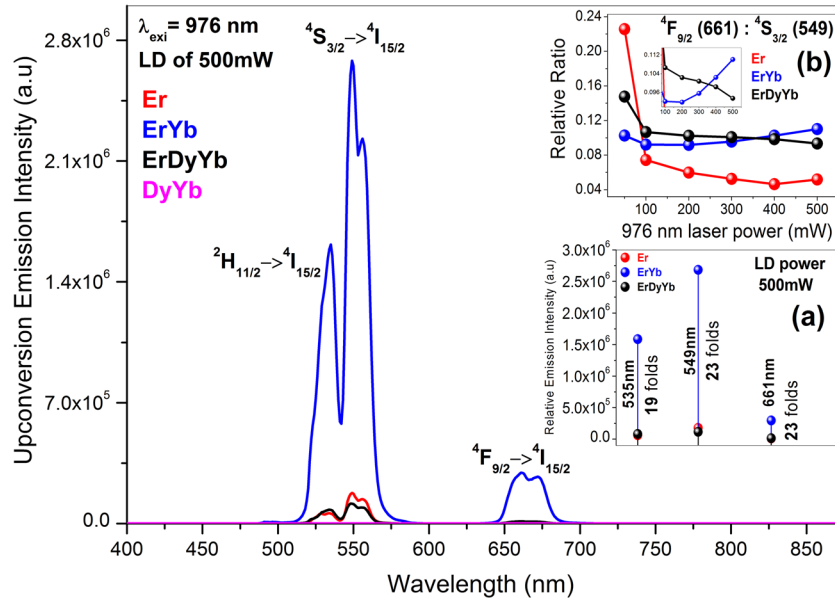
ErYb sample indicating the ET path (2) of ErDyYb is dominant over path (1). The decay times of Yb³⁺ and Er³⁺ ions in the presence of Dy³⁺ ions were presented in table 1 along with the estimated ET efficiencies (η_{ET} %). As depicted in the inset (a) of figure 4, the double exponential nature of decay profiles of 1006 nm is indicating the distribution of Yb³⁺ ions within or apart from the interaction sphere of Er³⁺/Dy³⁺ ions. Considering, the faster (τ_1) and slower (τ_2) decay times, the average lifetime (τ_{avg}) also calculated [45, 46] and presented in table 1. The Er³⁺ ~1.57 μ m emission decay time also greatly quenched in the triply doped sample as shown in the

inset (b) of figure 4 which is well fitted to a single exponential function similar to the Er and ErYb samples.

Although Pr³⁺ ions effectively mitigate the Vis-UC and ~1.5 μ m from Er³⁺ ions, Dy³⁺ ions not only act as an efficient quencher but also contribute to the bandwidth enhancement of MIR emission. In the present study, a ~60 fold reduction in the Er³⁺ ~1.57 μ m emission in the triply doped ErDyYb sample not only enhanced the MIR emission from Dy³⁺ ions (because of enhanced population at Dy³⁺:⁶H_{11/2} via efficient ET from Er³⁺:⁴I_{13/2} → Dy³⁺:⁶H_{11/2} state with an efficiency of ~78%) but also increased the bandwidth of MIR emission

Table 1. ET efficiency (η_{ET} %) calculated from measured lifetimes.

Sample	1006 nm lifetime (μ s)			1570 nm lifetime (ms)	η_{ET} (%)		η_{ET} (%)
	τ_1	τ_2	τ_{avg}		$Yb^{3+} \rightarrow Er^{3+}/Dy^{3+}$	$Er^{3+} \rightarrow Dy^{3+}$	
Yb	673.4 ± 3.1	—	—	—	—	—	—
Er	179.7 ± 2.7	—	—	3.062 ± 0.051	—	—	—
ErYb	69.3 ± 3.8	254.9 ± 3.1	215.4 ± 3.2	3.646 ± 0.034	89.7	68	—
DyYb	43.5 ± 1.3	182.4 ± 1.6	155.4 ± 1.4	—	93.5	76.9	—
ErDyYb	28.7 ± 1.6	108.2 ± 1.1	91.5 ± 1.3	0.798 ± 0.023	95.7	86.5	78.1

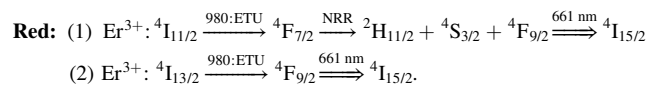
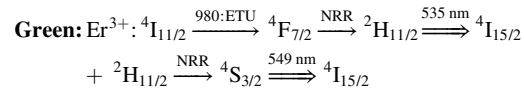
**Figure 5.** Vis-UC spectra of the samples upon 500 mW 976 nm laser diode excitation. Inset (a): relative ratio of red to green UC emission with variable pump intensity; inset (b): relative emission intensities of Vis-UC emissions of Er^{3+} ions in Er, ErYb and ErDyYb samples.

with high average peak intensity due to superimposition of Er^{3+} and Dy^{3+} MIR emission bands. Moreover, if we consider a reasonable average peak intensity ($\sim 0.5 \times 10^{-21} \text{ cm}^2$), the bandwidth can be stretched from $\sim 2600 \text{ nm}$ to $\sim 3100 \text{ nm}$ ($\sim 500 \text{ nm}$) which is highly beneficial to trace a small amount of environmental pollutants [1] which is a difficult task using conventional spectroscopic techniques. Again the ease of fiber drawing from these glass materials would be highly cost effective to develop compact solid state tunable MIR laser sources [2, 6].

Further, $Er^{3+}:^4I_{11/2}$ and $^4I_{13/2}$ levels acting as reservoir states for MIR as well as ETU based Vis-UC emissions, the close spectral overlap of $Er^{3+}:^4I_{11/2}$ with $Dy^{3+}:^6H_{7/2}$ state and $Er^{3+}:^4I_{13/2}$ with $Dy^{3+}:^6H_{11/2}$ may have a considerable effect on the MIR as well as Vis-UC emissions. To ascertain that, Vis-UC spectra have been recorded for Er, ErYb, ErDyYb and DyYb samples upon 976 nm diode laser with variable pump powers as shown in figure 5. Although there are reports on Vis-UC from Dy^{3+} doped systems [40, 47] which are mainly observed upon $\sim 800 \text{ nm}$ excitation. We have not observed any Vis-UC emission signature from Dy^{3+} ions neither in the Dy sample nor in the DyYb sample upon 976 nm excitation. On the other hand, the Vis-UC emission intensity of the ErYb

sample has increased many folds compared to the Er sample because of excellent resonance between $Yb^{3+}:^2F_{5/2}$ and $Er^{3+}:^4I_{11/2}$ excited states. However, in the presence of Dy^{3+} ions in the ErDyYb sample, a drastic ~ 23 fold reduction (at 500 mW power of laser diode) in the Er^{3+} : Vis-UC emission intensity has been observed (inset (a) of figure 5) due to the ET mechanism as stated for the ErDyYb sample.

The most prominent ETU process for Vis-UC emissions in Er/ErYb doped systems upon 980 nm excitation are given below [36–38]:



However, at higher pump powers/concentrations the ET path especially $Yb^{3+} \rightarrow Er^{3+}$ (upon 980 nm excitation) follows many other channels [48] that depend on the population density at different Er^{3+} ion excited states (contributing for ETU

process) which again strongly rely on the rare earth ion concentration, excitation wavelength, and source intensity. The relative ratio of red to green Vis-UC emission will give the depopulation rate at $\text{Er}^{3+}:^4\text{I}_{13/2}$ state for different excitation pump powers as shown in inset (b) of figure 5. For Er and ErYb samples, the relative ratio increases with an increase in the pump power indicating the ETU i.e. path (2) for red UC is increasing. On the other hand, the ErDyYb sample shows the gradually decreasing tendency of the ratio compared to Er and ErYb samples as depicted in the inset of inset (b) of figure 5 further confirming the depopulation or quenching of $\sim 1.5 \mu\text{m}$ emission via $\text{Er}^{3+}:^4\text{I}_{13/2} \rightarrow \text{Dy}^{3+}:^6\text{H}_{11/2}$ ET mechanism on account of $\text{Dy}^{3+}: \sim 2.95 \mu\text{m}$ emission enhancement which in turn helps to obtain a broad MIR emission on a combination of Er^{3+} and Dy^{3+} ions.

4. Conclusions

In this work, a broad (279 nm) MIR emission from an $\text{Yb}^{3+}/\text{Er}^{3+}/\text{Dy}^{3+}$ triply doped fluoro tellurite glass system (TBLAF) has been reported. Although Dy^{3+} ions singly doped and $\text{Dy}^{3+}\text{-Yb}^{3+}$ co-doped samples show a high bandwidth of $\sim 320 \text{ nm}$ which is broader than any Dy^{3+} ion-doped system so far, the emission intensity is not considerably high compared to fluoride/chalcogenide based glasses due to the dominant MPR from closely packed excited state of Dy^{3+} ions. However, in the triply doped glass system with considerable gain cross-section in the order of 10^{-21} cm^2 , the MIR emission bandwidth can be stretched from $\sim 2600 \text{ nm}$ to 3100 nm ($\sim 500 \text{ nm}$) which is practically not possible to obtain from Er^{3+} or Dy^{3+} singly doped systems. Dy^{3+} ions co-doping not only mitigates the Vis-UC emissions as well as prominent $\sim 1.5 \mu\text{m}$ emission from Er^{3+} ions but also contributes for the MIR emission bandwidth enhancement to a great extent.

Acknowledgment

The authors would like to thank the Director, Dr K Muraleedharan, CSIR-CGCRI for his encouragement and constant support. Authors would also like to acknowledge the support extended by Dr Ranjan Sen, Head, Glass Division.

References

- [1] Majid E-Z and Sorokina I T 2008 *Mid-Infrared Coherent Sources and Applications* (Dordrecht: Springer)
- [2] Godard A 2007 Infrared (2–12 μm) solid-state laser sources: a review *C. R. Phys.* **8** 1100–28
- [3] Vurgaftman I and Meyer J R 2006 Analysis of limitations to wallplug efficiency and output power for quantum cascade lasers *J. Appl. Phys.* **99** 123108
- [4] Mirov S B, Fedorov V V, Martyshkin D, Moskalev I S, Mirov M and Vasilyev S 2015 Progress in mid-IR lasers based on Cr and Fe-doped II–VI chalcogenides *IEEE J. Sel. Top. Quantum Electron.* **21** 1601719
- [5] Page R H, Schaffers K I, Deloach L D, Wilke G D, Patel F D, Tassano J B, Payne S A, Krupke W F, Chen K T and Burger A 1997 Cr^{2+} -doped zinc chalcogenides as efficient, widely tunable mid-infrared lasers *IEEE J. Quantum Electron.* **33** 609–17
- [6] Jackson S D 2012 Towards high-power mid-infrared emission from a fibre laser *Nat. Photon.* **6** 423–31
- [7] Tian Y, Xu R, Hu L and Zhang J 2012 Broadband 2.84 μm luminescence properties and Judd–Ofelt analysis in Dy^{3+} doped $\text{ZrF}_4\text{-BaF}_2\text{-LaF}_3\text{-AlF}_3\text{-YF}_3$ glass *J. Lumin.* **132** 128–31
- [8] Huang F, Ma Y, Li W, Liu X, Hu L and Chen D 2014 2.7 μm emission of high thermally and chemically durable glasses based on AlF_3 *Sci. Rep.* **4** 3607
- [9] Huang F, Guo Y, Ma Y, Zhang L and Zhang J 2013 Highly Er^{3+} -doped ZrF_4 -based fluoride glasses for 2.7 μm laser materials *Appl. Opt.* **52** 1399–403
- [10] Huang F, Tian Y, Li H, Xu S and Zhang J 2015 $\text{Ho}^{3+}/\text{Er}^{3+}$ co-doped fluoride glass sensitized by Tm^{3+} pumped by a 1550 nm laser diode for efficient 2.0 μm laser applications *Opt. Lett.* **40** 4297–300
- [11] Brekhovskikh M N and Fedorov V A 2014 IR-transparent glassy materials based on halides of group I–IV elements *Inorg. Mater.* **50** 924–9
- [12] Tokita S, Murakami M, Shimizu S, Hashida M and Sakabe S 2009 Liquid-cooled 24 W mid-infrared Er:ZBLAN fiber laser *Opt. Lett.* **34** 3062–4
- [13] Turnbull D A, Gu S Q and Bishop S G 1996 Photoluminescence studies of broadband excitation mechanisms for Dy^{3+} emission in $\text{Dy}:\text{As}_{12}\text{Ge}_{33}\text{Se}_{55}$ glass *J. Appl. Phys.* **80** 2436
- [14] Seddon A B, Tang Z, Furniss D, Sujecki S and Benson T M 2010 Progress in rare-earth-doped mid-infrared fiber lasers *Opt. Express* **18** 26704–19
- [15] Mid infrared transport fiber www.npphotonics.com/mid-infrared-transport-fibers-1-5-m
- [16] Wang W C, Yuan J, Li L X, Chen D D, Qian Q and Zhang Q Y 2015 Broadband 2.7 μm amplified spontaneous emission of Er^{3+} doped tellurite fibers for mid-infrared laser applications *Opt. Mater. Express* **5** 2964–77
- [17] Fan X, Li K, Li X, Kuan P, Wang X and Hu L 2014 Spectroscopic properties of 2.7 μm emission in Er^{3+} doped tellurite glasses and fibers *J. Alloys Compd.* **615** 475–81
- [18] Huang F, Ma Y, Liu L, Hu L and Chen D 2015 Enhanced 2.7 μm emission of Er^{3+} -doped low hydroxyl fluoroaluminate-tellurite glass *J. Lumin.* **158** 81–5
- [19] Yin D, Yang F, Wu L, Zhou Y, Zhou H and Wang X 2015 Enhanced 2.7 μm mid-infrared emission and energy transfer mechanism in $\text{Er}^{3+}/\text{Nd}^{3+}$ codoped tellurite glass *J. Alloys Compd.* **618** 666–72
- [20] Bai G, Ding J, Tao L, Li K, Hu L and Tsang Y H 2012 Efficient 2.7 micron emission from $\text{Er}^{3+}/\text{Pr}^{3+}$ codoped oxyfluorotellurite glass *J. Non-Cryst. Solids* **358** 3403–6
- [21] Gomes L, Milanese D, Lousteau J, Boetti N and Jackson S D 2011 Energy level decay processes in Ho^{3+} doped tellurite glass relevant to the 3 μm transition *J. Appl. Phys.* **109** 3–8
- [22] He J, Zhou Z, Zhan H, Zhang A and Lin A 2014 2.85 μm fluorescence of Ho-doped water-free fluorotellurite glasses *J. Lumin.* **145** 507–11
- [23] Balaji S, Gupta G, Biswas K, Ghosh D and Annapurna K 2016 Role of Yb^{3+} ions on enhanced $\sim 2.9 \mu\text{m}$ emission from Ho^{3+} ions in low phonon oxide glass system *Sci. Rep.* **6** 29203
- [24] Huang F, Hu L and Chen D 2014 Observation of 2.8 μm emission from diode-pumped Dy^{3+} -doped fluoroaluminate glasses modified by TeO_2 *Ceram. Int.* **40** 12869–73
- [25] Gomes L, Lousteau J, Milanese D, Mura E and Jackson S D 2014 Spectroscopy of mid-infrared (2.9 μm) fluorescence and energy transfer in Dy^{3+} -doped tellurite glasses *J. Opt. Soc. Am. B* **31** 429–35
- [26] Richards B D O, Teddy-Fernandez T, Jose G, Binks D and Jha A 2013 Mid-IR (3–4 μm) fluorescence and ASE studies in Dy^{3+} doped tellurite and germanate glasses and a fs laser inscribed waveguide *Laser Phys. Lett.* **10** 85802
- [27] Tian Y, Xu R, Hu L and Zhang J 2012 2.7 μm fluorescence radiative dynamics and energy transfer between Er^{3+} and

- Tm³⁺ ions in fluoride glass under 800 nm and 980 nm excitation *J. Quant. Spectrosc. Radiat. Transfer* **113** 87–95
- [28] Tian Y, Xu R, Zhang L, Hu L and Zhang J 2011 Observation of 2.7 μm emission from diode-pumped Er³⁺/Pr³⁺-codoped fluorophosphate glass *Opt. Lett.* **36** 109–11
- [29] Zhang L, Yang Z, Tian Y, Zhang J and Hu L 2011 Comparative investigation on the 2.7 μm emission in Er³⁺/Ho³⁺ codoped fluorophosphate glass *J. Appl. Phys.* **110** 1–7
- [30] Zhang P, Xu M, Zhang L, Hong J, Wang X, Wang Y, Chen G and Hang Y 2015 Intense 2.89 μm emission from Dy³⁺/Yb³⁺-codoped PbF₂ crystal by 970 nm laser diode pumping *Opt. Express* **23** 27786
- [31] Huang F, Liu X, Zhang Y, Hu L and Chen D 2014 Enhanced 2.7- and 2.84 μm emissions from diode-pumped Ho³⁺/Er³⁺-doped fluoride glass *Opt. Lett.* **39** 5917–20
- [32] Balaji S, Ghosh D, Biswas K, Gupta G and Annapurna K 2016 Experimental evidence for quantum cutting co-operative energy transfer process in Pr³⁺/Yb³⁺ ions co-doped fluorotellurite glass: dispute over energy transfer mechanism *Phys. Chem. Chem. Phys.* **18** 33115–25
- [33] Kaminskii A A 1990 *Laser Crystals: Their Physics and Properties* (Berlin: Springer-Verlag)
- [34] Zhang W, Lin J, Sun G, Jia Y, Zhao J, Ye S, Ren J and Rong L 2014 Stability, glass forming ability and spectral properties of Ho/Yb co-doped TeO₂–WO₃–ZnX (X = O/F₂/Cl₂) system *Opt. Mater.* **36** 1013–9
- [35] Zhang W, Lin J, Jia Y, Zhang S, Zhao J, Sun G, Ye S, Ren J and Rong L 2015 Enhanced 2–5 μm emission in Ho³⁺/Yb³⁺ codoped halide modified transparent tellurite glasses *Spectrochim. Acta A* **134** 388–98
- [36] Pokhrel M, Kumar G A, Balaji S, Debnath R and Sardar D K 2012 Optical characterization of Er³⁺ and Yb³⁺ co-doped barium fluorotellurite glass *J. Lumin.* **132** 1910–6
- [37] Desirena H, De la Rosa E, Shulzgen A, Shabet S and Peyghambarian N 2008 Er³⁺ and Yb³⁺ concentration effect in the spectroscopic properties and energy transfer in Yb³⁺/Er³⁺ codoped tellurite glasses *J. Phys. D: Appl. Phys.* **41** 95102
- [38] Jin Z, Nie Q, Xu T, Dai S, Shen X and Zhang X 2007 Optical transitions and upconversion luminescence of Er³⁺/Yb³⁺ codoped lead–zinc–tellurite oxide glass *Mater. Chem. Phys.* **104** 62–7
- [39] Hang P E Z, Hen Z H C, Ang Y I N H, Hen Z, In H A O Y, Hu S I Q I Z, Henhe S F U and Nming A L I 2016 Enhanced 2.7 μm mid-infrared emissions of Er³⁺ via Pr³⁺ deactivation and Yb³⁺ sensitization in LiNbO₃ crystal *Opt. Express* **24** 599–601
- [40] Li A-H, Lü Q, Zheng Z-R, Sun L, Wu W-Z, Liu W-L, Chen H-Z, Yang Y-Q and Lü T-Q 2008 Enhanced green upconversion emission of Er³⁺ through energy transfer by Dy³⁺ under 800 nm femtosecond-laser excitation *Opt. Lett.* **33** 693–5
- [41] Guo Y, Gao G, Li M, Hu L and Zhang J 2012 Er³⁺-doped fluoro-tellurite glass: a new choice for 2.7 μm lasers *Mater. Lett.* **80** 56–8
- [42] Jha A, Shen S and Naftaly M 2000 Structural origin of spectral broadening of 1.5 μm emission in Er³⁺-doped tellurite glasses *Phys. Rev. B* **62** 6215–27
- [43] Balaji S, Biswas K, Sontakke A D, Gupta G, Ghosh D and Annapurna K 2014 Al₂O₃ influence on structural, elastic, thermal properties of Yb³⁺ doped Ba–La–tellurite glass: evidence of reduction in self-radiation trapping at 1 μm emission *Spectrochim. Acta A* **133** 318–25
- [44] Nazabal V, Todoroki S, Nukui A, Matsumoto T, Suehara S, Hondo T, Araki T, Inoue S, Rivero C and Cardinal T 2003 Oxyfluoride tellurite glasses doped by erbium: thermal analysis, structural organization and spectral properties *J. Non-Cryst. Solids* **325** 85–102
- [45] Fujii T, Kodaira K, Kawauchi O, Tanaka N, Yamashita H and Anpo M 1997 Photochromic behavior in the fluorescence spectra of 9-anthrol encapsulated in Si–Al glasses prepared by the sol–gel method *J. Phys. Chem. B* **101** 10631–7
- [46] Sontakke A D, Biswas K, Mandal A K and Annapurna K 2010 Time resolved fluorescence and energy transfer analysis of Nd³⁺–Yb³⁺–Er³⁺ triply-doped Ba–Al–metaphosphate glasses for an eye safe emission (1.54 μm) *J. Fluoresc.* **20** 425–34
- [47] Kumar Rai V and Rai S B 2004 Optical transitions of Dy³⁺ in tellurite glass: observation of upconversion *Solid State Commun.* **132** 647–52
- [48] Berry M T and May P S 2015 Disputed mechanism for NIR-to-red upconversion luminescence in NaYF₄:Yb³⁺, Er³⁺ *J. Phys. Chem. A* **119** 9805–11